Physica Scripta. Vol. T59, 429–433, 1995

An Improved Pseudo Potential for the Two-Ion Paul Trap

M. G. Moore

Department of Physics, University of Arizona, Tucson, Arizona 85721, U.S.A.

and

R. Blümel

Department of Physics, State University of New York, Stony Brook, New York 11794-3800, U.S.A.

Received August 20, 1994; accepted December 15, 1994

Abstract

Keeping terms up to second order in the micro motion of two ions stored in a Paul trap we derive an improved two-ion pseudo potential which predicts crystal alignment effects that go beyond a standard pseudo-potential analysis and are supported by numerical evidence. The dynamical predictions can be checked experimentally with existing set-ups.

The Paul trap, originally designed as a practical tool for the three-dimensional confinement of charged particles [1, 2] has recently acquired the status of a micro lab for the investigation of nonlinear dynamics [3–8] and quantum chaos [9]. One of the most successful tools for discussing the dynamics of charged particles in a Paul trap is the pseudo-potential approximation [10]. The pseudo potential is obtained by averaging over the fast components of the ion motion, the so-called micro motion. The averaging procedure itself is generally applicable in nonlinear dynamics and is outlined in standard textbooks (see, e.g., [11–13]). The purpose of this paper is to refine and to extend this procedure to obtain an improved version of the two-ion pseudo potential by including terms up to second order in the micro motion of the trapped ions.

The standard pseudo potential $U_{eff}^{(s)}$ currently used in the literature [6, 14–16] and explicitly derived below is a composite consisting of the sum of the pseudo potentials of the individual ions and their mutual Coulomb interaction. New constants of the motion were found for the pseudo potential [6, 17]. Even the manifestations of classical chaos on the quantum level were analyzed on the basis of the standard pseudo potential [9]. But the question arises, how good this potential really is, and whether there are effects in the two-ion Paul trap which cannot be predicted on the basis of the standard pseudo potential.

In this note we derive an improved two-ion pseudo potential which predicts crystal alignment effects not contained in the standard pseudo potential $U_{eff}^{(s)}$. Therefore, while for some applications the potential $U_{eff}^{(s)}$ may be sufficiently accurate, it shows its limitations by failing to predict some basic two-ion phenomena. If the standard potential $U_{eff}^{(s)}$ is replaced by an improved pseudo potential to capture these phenomena, it raises the question what happens to the exactly integrable cases of $U_{eff}^{(s)}$ which were recently discussed intensively in the literature [14–18]. This is indeed a promising avenue for further research. Work on this topic is currently in progress.

On our way to the improved two-ion pseudo potential we will perform an even more ambitious task. We will derive a pseudo potential in full generality for the following set of two coupled dynamical equations

$$m\ddot{X} = -U_X(X, Z) - k_X X \cos(\omega t)$$
$$m\ddot{Z} = -U_Z(X, Z) - k_Z Z \cos(\omega t), \tag{1}$$

where $U_X = \partial U/\partial X$, $U_Z = \partial U/\partial Z$ and k_X, k_Z are constants. Since there are no restrictions on $U(X, Z)$ the pseudo potential derived from eq. (1) is applicable to a wide class of dynamical systems, the Paul trap being but a special case. The analysis of eq. (1) proceeds according to a method suggested by Kapiza [11]. Assuming that the cos (ωt) terms in eq. (1) are rapidly oscillating compared to the motion in the potential U alone, we split $X(t)$ and $Z(t)$ into a slowly and a rapidly varying component according to

$$X(t) = x(t) + \xi \cos(\omega t)$$
$$Z(t) = z(t) + \eta \cos(\omega t), \tag{2}$$

where ξ and η are the micro-motion amplitudes in the x and z direction, respectively. The micro-motion amplitudes are assumed to be constant during a cycle of the driving field, and change only slowly on the time scale of x and z, respectively. We will now assume that the micro-motion amplitudes are small, such that $U(X, Z)$ can be expanded up to second order in the micro-motion amplitudes according to

$$U(X, Z) = U(x, z) + U_x(x, z)\xi + U_z(x, z)\eta + \tfrac{1}{2}U_{xx}(x, z)\xi^2 + U_{xz}(x, z)\xi\eta + \tfrac{1}{2}U_{zz}(x, \eta)\eta^2, \tag{3}$$

where U_x, U_z, ... is shorthand for $\partial U/\partial x$, $\partial U/\partial z$, ..., respectively. Using eq. (3) in eq. (1) and equating cos (ωt) terms results in the following set of coupled linear equations for ξ and η

$$-m\omega^2\xi = -U_{xx}\xi - U_{xz}\eta - k_x x$$
$$-m\omega^2\eta = -U_{xz}\xi - U_{zz}\eta - k_z z. \tag{4}$$

Solving for ξ and η we obtain

$$\xi = [(m\omega^2 - U_{zz})k_x x + U_{xz}k_z z]/\Delta$$
$$\eta = [U_{xz}k_x x + (m\omega^2 - U_{xx})k_z z]/\Delta, \tag{5}$$

where $\Delta = (m\omega^2 - U_{xx})(m\omega^2 - U_{zz}) - U_{xz}^2$. Averaging the equations of motion (1) over one cycle of the driving field, we obtain

$$m\ddot{x} = -U_x - \tfrac{1}{4}\xi^2 U_{xxx} - \tfrac{1}{2}\xi\eta U_{xxz} - \tfrac{1}{4}\eta^2 U_{xzz} - \tfrac{1}{2}k_x\xi$$
$$m\ddot{z} = -U_z - \tfrac{1}{4}\xi^2 U_{xxz} - \tfrac{1}{2}\xi\eta U_{zzx} - \tfrac{1}{4}\eta^2 U_{zzz} - \tfrac{1}{2}k_z\eta. \quad (6)$$

It can be verified by direct differentiation that the above equations of motion can be derived from the potential

$$U_{eff}(x, z) = U(x, z) + \tfrac{1}{4}k_x x\xi(x, z) + \tfrac{1}{4}k_z z\eta(x, z). \quad (7)$$

We will now show that the equations of motion of two identical ions in a Paul trap are indeed a special case of eq. (1). Denoting by $\boldsymbol{r}_1$ and $\boldsymbol{r}_2$ the positions of the two ions in the trap, we introduce their relative separation $\boldsymbol{\rho} = \boldsymbol{r}_1 - \boldsymbol{r}_2$ and the position of the center of mass $\boldsymbol{R} = (\boldsymbol{r}_1 + \boldsymbol{r}_2)/2$. In the case of identical ions it was shown by many authors that the Paul trap dynamics is separable in $\boldsymbol{\rho}$ and $\boldsymbol{R}$ (see, e.g, [3]). The center of mass $\boldsymbol{R}$ satisfies a simple single particle Mathieu equation [19] and is of no dynamical interest. Stable trapping is achieved inside the Mathieu stability region [1, 2] shown as the regions framed by the full lines in Fig. 1. The interesting dynamics happens in the relative motion $\boldsymbol{\rho} = (X, Y, Z)$ of the two ions. In the presence of laser cooling with a well-aligned laser the z component of the angular momentum is "frozen out". Then, due to the axial symmetry of the trap, the y axis of the coordinate system can always be chosen such that $Y \equiv 0$ for all time and the X and Z components of $\boldsymbol{\rho}$ suffice for the description. In suitable dimensionless units [8] the equations of motion are given by

$$\ddot{X} = -[a + 2q\cos(2t)]X + X/\rho^3$$
$$\ddot{Z} = 2[a + 2q\cos(2t)]Z + Z/\rho^3, \quad (8)$$

where $\rho = (X^2 + Z^2)^{1/2}$. The set (8) is obtained from eq. (1) with $m = 1$, $\omega = 2$, $k_x = 2q$, $k_z = -4q$ and

$$U(x, z) = ax^2/2 - ax^2 + 1/r, \quad (9)$$

where $r = (x^2 + z^2)^{1/2}$.

In order to calculate the potential U_{eff} explicitly, we need the partial derivatives of U. They are easily calculated resulting in

$$U_x = ax - x/r^3, \quad U_z = -2az - z/r^3,$$
$$U_{xx} = a - 1/r^3 + 3x^2/r^5, \quad U_{xz} = 3xz/r^5,$$
$$U_{zz} = -2a - 1/r^3 + 3z^2/r^5. \quad (10)$$

Using these expressions, the pseudo potential (7) is given explicitly by

$$U_{eff} = \frac{1}{r} + \tfrac{1}{2}ax^2 - az^2 + N/D, \quad (11)$$

where

$$N = Gq^2x^2 - 12q^2x^2z^2/r^5 + 4Hq^2z^2,$$
$$D = GH - 9x^2z^2/r^{10} \quad (12)$$

and

$$G = 4 + 2a + (x^2 - 2z^2)/r^5,$$
$$H = 4 - a + (z^2 - 2x^2)/r^5. \quad (13)$$

Since the analytical structure of eq. (11) is complicated, we discuss two approximations to eq. (11). The standard pseudo potential $U_{eff}^{(s)}$ is obtained by assuming $a, q^2 \ll 1$. This results in

$$U_{eff}^{(s)} = \frac{1}{r} + \tfrac{1}{2}\mu_x^2 x^2 + \tfrac{1}{2}\mu_z^2 z^2, \quad (14)$$

where $\mu_x = (a + q^2/2)^{1/2}$ and $\mu_z = [2(q^2 - a)]^{1/2}$ are the dimensionless single ion pseudo oscillator frequencies in x and z direction, respectively. Especially for very small a and q the standard pseudo potential $U_{eff}^{(s)}$ captures many of the important features of two-ion dynamics and crystallization [3–6, 9, 20–23] and was the basis of many investigations in the current literature (see, e.g., [6, 9, 16]).

A better approximation to eq. (11) can be obtained by expanding the N/D term in eq. (11) up to first order in 1/length. The result is

$$\tilde{U}_{eff} = \frac{1}{r} + \frac{2q^2 + 4a - a^2}{2(4 - a)}x^2 + \frac{2q^2 - 2a - a^2}{2 + a}z^2 + \frac{q^2}{r^5} \times \left[\frac{2x^4}{(4 - a)^2} + \frac{2z^4}{(2 + a)^2} - \frac{4(17 + 2a - a^2)x^2z^2}{(4 - a)^2(2 + a)^2}\right]. \quad (15)$$

The potential (15) looks much more complicated than the standard pseudo potential (14). The question is whether eq. (15) is just simply more accurate than eq. (14) or whether eq. (15) predicts qualitatively new physics not contained in eq. (14). The latter is the case since eq. (15) predicts a qualitatively new regime of crystal orientations that cannot be obtained from eq. (14).

If a two-ion crystal is cooled to its minimal energy configuration, its slow coordinates x and z will be found to correspond closely to a minimum in the pseudo potential. In other words, the pseudo-potential minima determine the crystal equilibrium configurations.

In order to find the possible crystal orientations according to the standard pseudo potential (14), all we have to do is to solve the coupled equations $\partial U_{eff}^{(s)}(x, z)/\partial(x, z) = 0$. They are given explicitly by

$$\frac{\partial U_{eff}^{(s)}}{\partial x} = \left[-\frac{1}{r^3} + \mu_x^2\right]x = 0,$$
$$\frac{\partial U_{eff}^{(s)}}{\partial z} = \left[-\frac{1}{r^3} + \mu_z^2\right]z = 0. \quad (16)$$

In order to check whether a solution of eq. (16) indeed corresponds to a minimum, we also need the set of second derivatives of $U_{eff}^{(s)}$. They are given by

$$\frac{\partial^2 U_{eff}^{(s)}}{\partial x^2} = \frac{2x^2 - z^2}{r^5} + \mu_x^2, \quad \frac{\partial^2 U_{eff}^{(s)}}{\partial x \partial z} = \frac{3xz}{r^5},$$
$$\frac{\partial^2 U_{eff}^{(s)}}{\partial z^2} = \frac{2x^2 - x^2}{r^5} + \mu_z^2. \quad (17)$$

Because of the Coulomb singularity, $(x = 0, z = 0)$ is not a solution of eq. (16). This leaves three cases:

(i) $x = 0, z \neq 0$

In this case we have $z = \mu_z^{-2/3}$. The mixed derivative in eq. (17) vanishes identically in this case. The second derivative with respect to z equals $3\mu_z^2$ and is positive. The second derivative with respect to x yields $\mu_x^2 - \mu_z^2$. It is positive and

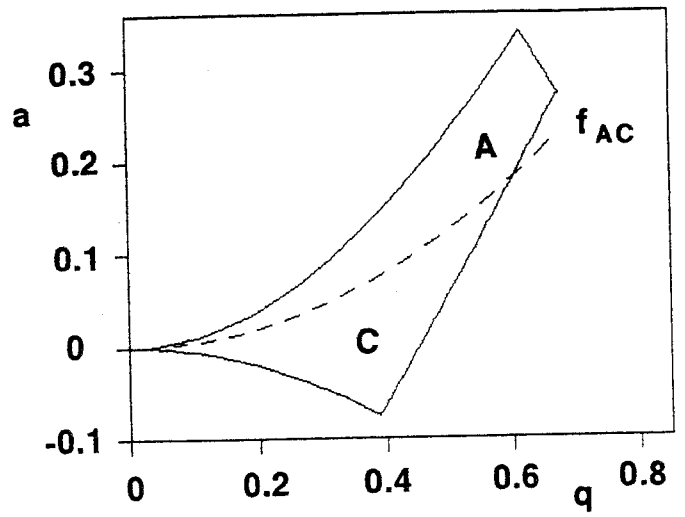

Fig. 1. Orientation regions for two-ion crystals in a Paul trap predicted by the standard pseudo potential $U^{(s)}_{eff}$. The full lines frame the single ion Mathieu stability region. The dashed lines show the analytically determined border-line function f_{AC} between regions A (z alignment) and region C (x alignment).

corresponds to a minimum for $a > q^2/2$. This condition defines a whole region (denoted by A in Fig. 1) inside the Mathieu stability diagram [1, 2]. In region A the two-ion crystal is aligned with the z axis.

(ii) $x \neq 0, z = 0$

This case is analogous to case (i). The mixed derivative vanishes, the second derivative with respect to x is positive and the presence of a minimum requires $\mu_z^2 - \mu_x^2 > 0$ which implies $a < q^2/2$. The corresponding region in the Mathieu stability diagram is denoted by C (see Fig. 1). In region C the crystal is aligned to the x axis.

(iii) $x \neq 0, z \neq 0$

In this case, we must have simultaneously $r^3 = 1/\mu_x^2$ and $r^3 = 1/\mu_z^2$. This is possible only for $\mu_x = \mu_z$, i.e., in case the potential (14) is spherical. This condition yields $a = q^2/2$ and forms the border-line between regions A and C. We denote the border-line function by $q = f_{AC}(a) = \sqrt{2a}$ (dashed line in Fig. 1). Points on f_{AC} do not correspond to minima since the matrix of second derivatives is not positively definite.

As a result of this analysis we obtain that for a generic choice of control parameters a and q the two-ion crystal can be found either aligned with the z axis or aligned with the x axis. Except for a set of zero area of a and q values (i.e., for points that satisfy f_{AC}) there is no third possibility. This case, however, is "soft" and provides no angular restoring force.

We will now investigate crystal orientations predicted by the potential (15). This time the analysis is somewhat more difficult but can still be performed analytically with no approximations. We will see below that the potential (15) predicts that the zero area border-line $q = f_{AC}(a)$ widens to a finite area located between A and C and denoted by B. Therefore, there are "real" minima in region B which correspond to nontrivial crystal orientations with an angular restoring force. In order to calculate the border-lines f_{AB} and f_{BC} between the three orientation regions we will first look for minima on the x and z axis, respectively, and then determine where those minima, as a function of a and q lose stability. The onset of instability marks the borders between A and B, and B and C, respectively.

A minimum on the x axis is given by

$$\frac{\partial \tilde{U}_{eff}(x, z = 0)}{\partial x} = 0. \tag{18}$$

This equation can be solved analytically and yields

$$x = \left[\frac{2q^2 + (4 - a)^2}{(2q^2 + 4a - a^2)(4 - a)}\right]^{1/3}. \tag{19}$$

This minimum loses stability in z direction at

$$\frac{\partial^2 \tilde{U}_{eff}(x, z = 0)}{\partial z^2} = \frac{4q^2 - 4a - 2a^2}{2 + a} - \frac{1}{x^3} \times \left[1 + \frac{10q^2}{(4 - a)^2} + \frac{8(17 + 2a - a^2)q^2}{(4 - a)^2(2 + a)^2}\right] = 0. \tag{20}$$

Using eq. (19) in eq. (20), we see that eq. (20) becomes a quadratic equation in q^2 given by

$$\alpha q^4 + \beta q^2 + \varepsilon = 0, \tag{21}$$

where the coefficients in eq. (21) are given by

$$\alpha = -48(a^2 + 8a + 24), \quad \beta = 96(4 - a)(4 - 9a - 4a^2),$$
$$\varepsilon = -6a(4 - a)^3(4 + 2a)(a + 2). \tag{22}$$

The solution of eq. (21) is given by

$$q = f_{BC}(a) = \sqrt{-\frac{\beta}{2\alpha} + \frac{1}{2\alpha}\sqrt{\beta^2 - 4\alpha\varepsilon}}. \tag{23}$$

It marks the boundary between regions C and B. The function f_{BC} is shown as the bottom dashed line in Fig. 2.

The minima on the z axis are given by

$$\frac{\partial \tilde{U}_{eff}(x = 0, z)}{\partial z} = 0. \tag{24}$$

Just like the corresponding equation for minima on the x axis this equation can again be solved analytically and

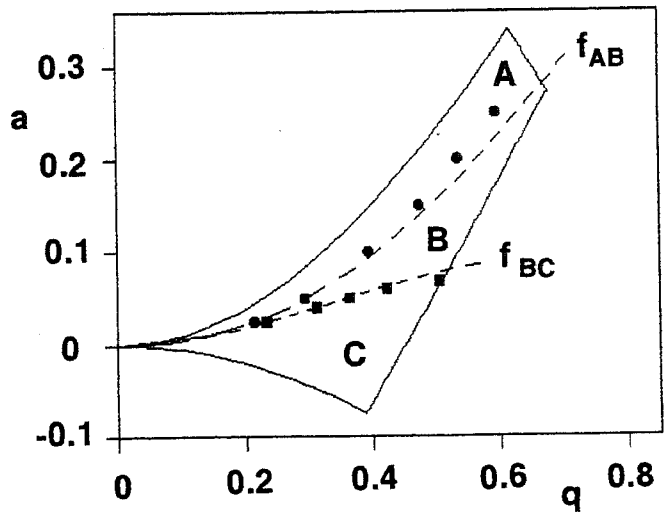

Fig. 2. Crystal orientation regions predicted by the improved pseudo potential $\tilde{U}_{eff}$. Shown are the analytical predictions f_{AB} and f_{BC} (dashed lines) for the A/B boundary and the B/C boundary, respectively. Numerical results for the location of the A/B boundary (full dots) and the B/C boundary (full squares) are also shown.

yields

$$z = \left[\frac{2q^2 + (2+a)^2}{2(2+a)(2q^2 - 2a - a^2)}\right]^{1/3}. \tag{25}$$

The minima lose stability in x direction at

$$\frac{\partial^2 \tilde{U}_{eff}(x=0, z)}{\partial x^2} = \frac{2q^2 + 4a - a^2}{4 - a} - \frac{1}{z^3} \times \left[1 + \frac{10q^2}{(2+a)^2} + \frac{8(17 + 2a - a^2)q^2}{(4-a)^2(2+a)^2}\right] = 0. \tag{26}$$

Again, eq. (26) is equivalent with a quadratic equation in q^2 of the form (21) when using the location of the minima (25). This time the coefficients in eq. (21) are given by

$$\alpha = -12(a^2 - 22a + 96),$$
$$\beta = -24(2+a)(5a^2 - 27a + 4),$$
$$\varepsilon = 3a(4-a)^2(2+a)^3, \tag{27}$$

and the solution of eq. (21) with these coefficients is given by

$$q = f_{AB}(a) = \sqrt{-\frac{\beta}{2\alpha} - \frac{1}{2\alpha}\sqrt{\beta^2 - 4\alpha\varepsilon}}. \tag{28}$$

This solution looks similar to eq. (23), but note the reversed sign under the square root. The function (28) defines f_{AB}, the boundary between regions A and B. It is shown as the upper dashed line in Fig. 2.

Excellent explicit expressions for $a = f_{AB}^{-1}(q)$ and $a = f_{BC}^{-1}(q)$ can be obtained by first expanding the pseudo potential (15) to first order in a and then repeating the steps that led to the conditions (20) and (26). For the expanded pseudo potential we obtain

$$U_{eff}^{(app)} = \frac{1}{r} + \left(\frac{a}{2} + \frac{q^2}{4} + \frac{aq^2}{16}\right)x^2 + \left(q^2 - a - \frac{aq^2}{2}\right)z^2 + \frac{q^2}{r^5} \times \left[\frac{2+a}{16}x^2 + \frac{1-a}{2}z^4 - \frac{34 - 13a}{32}x^2z^2\right]. \tag{29}$$

The explicit approximate expression for f_{AB}^{-1} is then given by

$$f_{AB}^{-1}(q) \approx \frac{\tilde{\alpha} - (\tilde{\beta})^{1/2}}{\tilde{\varepsilon}}, \tag{30}$$

where $\tilde{\alpha} = 59q^4 + 58q^2 + 16$, $\tilde{\beta} = 25q^8 - 1028q^6 + 4036q^4 + 1856q^2 + 256$, $\tilde{\varepsilon} = 36q^4 + 76q^2$. The corresponding expression for f_{BC}^{-1} is given by

$$f_{BC}^{-1} \approx \frac{\tilde{\varepsilon}}{\tilde{\alpha} + (\tilde{\beta})^{1/2}}, \tag{31}$$

where this time $\tilde{\alpha}$, $\tilde{\beta}$ and $\tilde{\varepsilon}$ are given by $\tilde{\alpha} = q^4 + 44q^2 + 32$, and $\tilde{\beta} = q^8 + 280q^6 + 1744q^4 + 2816q^2 + 1024$, and $\tilde{\varepsilon} = 32q^2 - 24q^4$. The accuracy of eqs (30) and (31) is better than 5% over the whole Mathieu stability region.

In region B the minima of the pseudo potential (11) are not located on one of the axes of the trap. This means that within the pseudo-potential approximation (11) a two-ion crystal in region B forms an angle $\bar{\psi}(a, q)$ with the z axis of the trap that is different from 0 or $\pi/2$. The standard pseudo potential does not predict region B, Thus, the improved pseudo potential $\tilde{U}_{eff}$ predicts new properties of two-ion crystals in the Paul trap. The pseudo potential (11) describes new physics which is not contained in $U_{eff}^{(s)}$.

But how exactly does region B manifest itself in an experiment that tries to verify its existence? First of all we have to acknowledge that the pseudo potential (11), as any other pseudo potential, describes only the time-averaged motion on a time scale longer than one period of the driving field. If the micro motion is taken into account, the two-ion crystal is not locked into a stationary orientation $\bar{\psi}$ but (apart from a radial oscillation) executes a vibration around $\bar{\psi}$. This is explained considering the eqs (5) for the micro-motion amplitudes ξ and η. Since eq. (5) is a nonlinear transformation from (x, z) to (ξ, η), the micro motion will possess radial as well as angular components, and will in general not correspond to a purely radial vibration. The angular vibration about $\bar{\psi}$ together with the crystal nonalignment is a tell-tale signal for the experimental identification of region B. Since the pseudo potential resulted from averaging over the micro motion, $\bar{\psi}$ can be calculated immediately from the location of the pseudo-potential minimum for given a and q. This result, too, can be compared with the experimentally determined average orientation of a two-ion crystal and provides a further test for the existence and the shape of region B.

We are not aware of any attempts at an experimental investigation of region B. In the absence of experimental data the best we can do is to compare the analytical predictions with numerical simulations. In order to model laser cooling, we added damping terms to the equations of motion (8) resulting in the following modified equations of motion

$$\ddot{X} = -[a + 2q\cos(2t)]X - \gamma\dot{X} + X/\rho^3$$
$$\ddot{Z} = 2[a + 2q\cos(2t)]Z - \gamma\dot{Z} + Z/\rho^3. \tag{32}$$

First, we check the border-lines f_{AB} and f_{BC} between the three orientation regions. For $\gamma = 10^{-4}$ we integrated the set (32) using a numerical fourth-order Runge–Kutta scheme [24] with constant step size. Since f_{AB} marks the onset of crystal nonalignment with the z axis, we solved the set (32) on various constant-a paths in the Mathieu stability region. We started the integration close to the left-hand stability border. After obtaining a two-ion crystal, this configuration was dragged [7] adiabatically toward f_{AB} by increasing q slowly over close to a million cycles of eq. (32) while keeping a constant. During this procedure, the orientation of z was constantly checked. As soon as the crystal started to misalign, we stopped the integration and marked the result with a full dot in Fig. 2. This procedure was repeated for several other a values (see full dots in Fig. 2). The agreement with the analytical border f_{AB} is very good. An analogous procedure was used to determine the border f_{BC}. This time we marked the points corresponding to the onset of reorientation with a full square. Again, the numerical results are very close to the analytical prediction.

Another "numerical experiment" concerned the computation of the average orientation angle $\bar{\psi}$. This time we chose $\gamma = 10^{-3}$. The task was to integrate eq. (32) numerically on an equispaced grid with $\Delta a = \Delta q = 0.01$ and to compute numerically $\bar{\psi}(a, q)$. The procedure was as follows. For a given grid point (a_j, q_k) we selected a large $\gamma \gg 10^{-3}$ and an

arbitrary set X, Z, $\dot{X}$, $\dot{Z}$ of initial conditions and integrated the set (32) long enough to obtain a stable two-ion crystal. Then, we adiabatically reduced γ to its final value $\gamma = 10^{-3}$. This way we obtained initial conditions which correspond to a two-ion crystal at $\gamma = 10^{-3}$. Finally, we integrated eq. (32) over one more micro-motion cycle to obtain $\psi(a_j, q_k; t)$ and computed its time average $\bar{\psi}(a_j, q_k)$. Figure 3(a) shows the resulting $\bar{\psi}$ values in the form of line segments at the positions (a_j, q_k) in the (a, q) stability diagram of the Paul trap. The inclinations of the line segments represent the values of the average orientation angles $\bar{\psi}$ of the crystal in x–z space. A region at the right-hand border of the stability diagram is empty. The reason is that no two-ion crystals exist in this region and $\bar{\psi}$ is not defined [7]. In order to compare the numerical results with the predictions according to $\tilde{U}_{eff}$ we have to determine the minima of $\tilde{U}_{eff}$ in region B. We have not yet found a way to do this analytically. Therefore, since this task has to be done numerically there was no difference in computing time between finding minima for $\tilde{U}_{eff}$ or for the full pseudo potential U_{eff}. Figure 3(b) shows the corresponding equilibrium angles derived from the positions x_m and z_m of the pseudo-potential minima according to

$$\bar{\psi} = \arctan(z_m/x_m). \tag{31}$$

Very good agreement is obtained between the predictions of $\bar{\psi}$ obtained from the exact dynamics (32) [see Fig. 3(a)] and the predictions for $\bar{\psi}$ according to U_{eff} [see Fig. 3(b)].

Neither the standard pseudo potential $U^{(s)}_{eff}$ nor the improved pseudo potential (11) predict the stability borders to the right and on top of the Mathieu stability region. In order to indicate this fact, Fig. 3(b) shows that on the basis of U_{eff} alone, orientation angles can be defined extending beyond the Mathieu stability region.

We also computed numerically the border-lines g_{AB} and g_{BC} predicted by the full pseudo potential (11) for the A/B border and the B/C border, respectively. We found that both f_{AB} and f_{BC} are identical with g_{AB} and g_{BC} on the scale of Fig. 2. This shows that $\tilde{U}_{eff}$ is an excellent approximation to U_{eff}.

We are confident that ion trapping experiments [3–6, 21, 22] or experiments with charged micro spheres [8] will soon confirm the existence of region B.

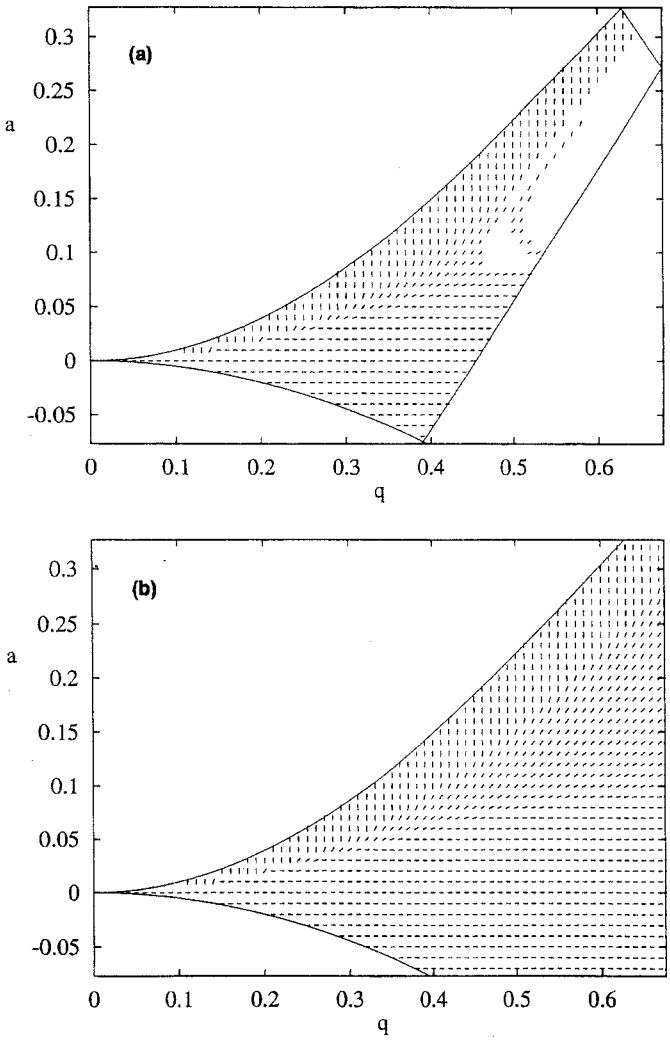

Fig. 3. Time-averaged field of orientation line segments for a two-ion crystal with trap control parameters a and q. (a) Numerical result, (b) orientations obtained from the improved pseudo potential U_{eff}.

References

1. Paul, W., Osberghaus, W. and Fischer, E., Forschungsber. Wirtsch. Verkehrsminist. Nordrhein Westfalen **415**, 1 (1958).
2. Paul, W., Rev. Mod. Phys. **62**, 531 (1990).
3. Hoffnagle, J., DeVoe, R. G., Reyna, L. and Brewer, R. G., Phys. Rev. Lett. **61**, 255 (1988).
4. Blümel, R. *et al.*, Nature **334**, 309 (1988).
5. Brewer, R. G., Hoffnagle, J. and DeVoe, R. G., Phys. Rev. Lett. **65**, 2619 (1990).
6. Blümel, R., Kappler, C., Quint, W. and Walther, H., Phys. Rev. **A40**, 808 (1989).
7. Emmert, J. W., Moore, M. and Blümel, R., Phys. Rev. **A48**, R1757 (1993).
8. Hoffnagle, J. and Brewer, R. G., Phys. Rev. Lett. **71**, 1828 (1993).
9. Moore, M. and Blümel, R., Phys. Rev. **A48**, 3082 (1993).
10. Dehmelt, M., in "Advances in Atomic and Molecular Physics" (Edited by D. R. Bates and I. Estermann) (Academic Press, New York 1967), Vol. 3, p. 53.
11. Landau, L. D. and Lifschitz, E. M., "Mechanik" (Vieweg, Braunschweig 1970).
12. Lichtenberg, A. J. and Lieberman, M. A., "Regular and Stochastic Motion" (Springer, New York 1983).
13. Sagdeev, R. Z., Usikov, D. A. and Zaslavsky, G. M., "Nonlinear Physics" (Harwood Academic, Chur 1988).
14. Baumann, G., Phys. Lett. **A162**, 464 (1992).
15. Baumann, G. and Nonnenmacher, T. F., Phys. Rev. **A46**, 2682 (1992).
16. Farrelly, D. and Howard, J. E., Phys. Rev. **A49**, 1494 (1994).
17. Blümel, R., Phys. Rev. **A48**, 854 (1993).
18. Blümel, R., Phys. Lett. **A174**, 174 (1993).
19. Abramowitz, M. and Stegun, I. A., "Handbook of Mathematical Functions" (National Bureau of Standards, Washington, DC 1964).
20. Wuerker, R. F., Shelton, H. and Langmuir, R. V., J. Appl. Phys. **30**, 342 (1959).
21. Diedrich, F., Peik, E., Chen, J. M., Quint, W. and Walther, H., Phys. Rev. Lett. **59**, 2931 (1987).
22. Wineland, D. J., Bergquist, J. C., Itano, W. M., Bollinger, J. J. and Manney, C. H., Phys. Rev. Lett. **59**, 2935 (1987).
23. Schiffer, J. P. and Kienle, P., Z. Phys. **A321**, 181 (1985).
24. Braun, M., "Differential Equations and Their Applications" (Springer, New York 1975).